LBL- 23092

FABRICATION AND 35GH$_Z$ TESTING OF KEY TWO-BEAM ACCELERATOR COMPONENTS

D.B. Hopkins, G.W. Koehler, R.W. Kuenning, W. Low, A.M. Sessler
Lawrence Berkeley Laboratory, University of California
Berkeley, CA. 94720

D. Prosnitz, A.L. Throop, G.R. Westenskow
Lawrence Livermore National Laboratory
P.O. Box 808, L-626
Livermore, CA 94550

J. Haimson
Haimson Research Corporation
4151 Middlefield Road
Palo Alto, CA 94303

Abstract

This paper discusses two 34-cavity 10-cm long, 33.3 GH$_Z$ high gradient accelerator sections fabricated by different methods. Also described are the construction and testing of a septum coupler designed for periodically extracting power from the free electron laser (FEL) portion of a two-beam accelerator.

Introduction

The two-beam accelerator is a very promising candidate for achieving the ultra-high electron energies (e.g. $\geq$ 1 TeV) required in next-generation linear colliders.[1-3] A portion of the TBA is shown in Figure 1. In 1985, a seven-cell high gradient structure (HGS) was constructed and tested at ELF[4] at 34.6 GH$_Z$.[2] It was fabricated by the electroform technique. With only routine metallurgy and relatively poor vacuum involved (~10^{-5} to 10^{-4} Torr), the HGS achieved a peak surface electric field gradient of ~ 380 MV/m during a 3.1 MW, 10-15 ns pulse. This would correspond to an average accelerating gradient of ~ 190 MV/m in an actual accelerator. Encouraged by this result, we began the construction of two identical high-quality accelerator sections using different techniques. The first was fabricated using the machine-and-braze technique. The second was to employ the electroforming approach. We hoped to comparison-test the two at ELF and determine whether or not either was markedly superior to the other insofar as ultimate gradients were concerned. Also it appeared that the electroforming approach might significantly simplify the fabrication of these sections. The starting points for the HGA design were our requirements for (1) a filling time of ~ 15 ns, compatible with the ELF pulse width, (2) ~ 33.31 GH$_Z$ operating frequency, centered in the tuning range of the magnetron driving ELF, (3) a $2\pi/3$ mode, v_p = c, nearly constant-gradient disc-loaded waveguide structure[5], for easy comparison to existing lower frequency accelerators, and (4) radial pumpout holes in the walls of each cavity in order to maintain $\lesssim 10^{-7}$ Torr vacuum levels.

Machined and Brazed HGA

Under contract, the Haimson Research Corporation (HRC) produced the detailed design and carried out the fabrication of the machined and brazed HGA. This work is described in a companion paper[6]. A simplified diagram of the disc-loaded waveguide structure is shown in Figure 1 of this reference. The Haimson design results in a nominally 10cm-long structure of 34 cavities, an iris diameter from 0.10254 inches to 0.08540 inches and a corresponding cavity diameter range from 0.28619 inches to 0.28100 inches. The tolerance on all critical dimensions is ± 50 microinches (± 1.25 micrometers). The HGA is vacuum-jacketed and pumped by a Vacion appendage pump. The completed assembly after bakeout and sealing is shown mounted to a strongback in Figure 2. HRC fabricated the HGA brazed microwave structure and couplers, the tapered E-bend matched transition waveguides with oversize WR28 flanges, the brazed alumina windows in WR187 oversize waveguide, the stainless steel combination high vacuum and microwave flanges and the strongbacks. LBL/LLNL supplied the electroformed adapter and pump-out tapers, each of which has an attached 2 ℓ/s Vacion appendage pump. All of the accelerator subassemblies except the tapers were oven brazed at temperatures in the range of 1040 to 860°C and after final microwave tuning and matching, the overall assembly was baked out at 250°C, sealed off and delivered under vacuum. It is being maintained at a vacuum level in the 10^{-9} Torr range while awaiting a high-power microwave source for testing. This should be available in less than a year. The HGA is expected to achieve an average accelerating gradient in the few hundred MV/m range. The relationship between accelerating gradient and power is given by $E_{acc} = 31.0\sqrt{P(MW)}$ MV/m; the maximum surface field on a disc iris is $66.8\sqrt{P(MW)}$ MV/m.

Electroformed HGA

In a collaborative effort between LBL, LLNL, and the Sandia National Laboratory, Livermore (SNLL), an electroforming process has been developed for fabricating an HGA. This work is discussed in a companion paper[7] and elsewhere[8]. Our goal was to produce an HGA having the same dimensions and mechanical tolerances as were achieved in the brazed HGA. Input and output microwave couplers identical to those of the brazed HGA were fabricated by HRC. These were to have been joined to the HGA by electroplating. A variety of copper-plating studies was conducted to achieve our requirements for (1) low porosity, inclusions and grain size, (2) precisely replicated mandrel surface, and (3) negligible void formation and outgassing at bakeout temperatures as high as 450°C. Additionally, machining methods for producing the deeply slotted aluminum mandrels were investigated. Figure 3 shows a mandrel section and finished HGA prototype alongside a centimeter scale. The final design calls for wider longitudinal strengthening ribs into which cavity radial pumpout holes and tuner access ports are drilled. The standard 6061-T6 aluminum alloy was used for the mandrel material. A dc cyanide plating process produced optimum results when operated at a current density of 4 A/ft^2 and a mandrel rotation rate of 10 rpm. Grain size and outgassing rate were acceptable and void

This work was supported by the Office of Energy Research, High Energy Physics Division of the U.S. Department of Energy Under Contract No. DE-AC03-76SF00098. Performed jointly under the auspices of the U.S. Department of Energy by the Lawrence Livermore National Laboratory under W-7505-ENG-48, and by the Sandia National Laboratory, Livermore, under DE-AC04-76DP00789.

formation was negligible when samples were baked at 650°C. Budget restrictions made it necessary to discontinue this work before a final HGA could be completed. A number of acceptable mandrels have been produced as well as the couplers and HGA vacuum manifold and windows.

Septum Coupler Design and Fabrication

The origin of the septum coupler concept is discussed elsewhere[2]. Figure 4 shows a cross-sectional diagram of the type of test section we have constructed and tested at ELF. The microwave E-vector of the TE_{01} mode lies vertically in the plane of the paper; power flow is from left to right. The dimensions shown are in inches (centimeters). The spacing between the leading edges of the first and second pairs of septa is six inches. A number of geometric and electrical constraints essentially fixed all of the key dimensions of the coupler. Taking advantage of the TE_{01} mode symmetry plane, the coupler was fabricated in two halves by a numerically controlled milling machine. These halves were later TIG-welded together. Figure 5 shows the two halves. The material chosen for the coupler was 310S stainless steel. Individual wall thicknesses were held to 0.062 in. Stress calculations[9] indicated that the maximum broad-wall deflection under vacuum loading would be about 0.021 in.

Septum Coupler Testing

The techniques employed for high-power microwave measurements at ELF have been described previously[3,4]. For the septum coupler, calibration measurements on a test bench and in position following the wiggler at ELF established both the relatively good symmetry of power coupled out by both oppositely-paired septa and the attenuation through the five coupled arms. However, these tests revealed that the second pair of septa only coupled out about a third of the expected power. We conclude that in this largely oversized guide the tapering between the first and second septum pairs is too abrupt. We assign a general 3 dB uncertainty ("error bar") to the FEL power measurement. Also, the calibrations were conducted with 10-20 ns microwave pulses. This avoided resonant absorption peaks, caused by mode conversion, that arise during long-pulse or c.w. excitation of oversized waveguide systems.

Figure 6 shows the power measurement nomenclature and the locations for magnetic field measurements. Test results will be summarized here; they are described in detail elsewhere[10]. The ELF operating frequency was 35.0 GH_z. In the first tests, the septum coupler was placed after the ELF wiggler and beam dump. Power from the five coupler outputs passed through separate vacuum-pumped diffraction-loss chambers which introduced ~ 40 to 50 dB loss into each line so that the remaining power could be handled and measured by standard components. We wished to study the symmetry and stability of power division, stability of relative phase, relative higher mode content, and arcing thresholds. The value for P_O is inferred from the measured P_{SO} value and the previously measured value for the loss straight through the coupler, typically ~ 1.3 dB.

Allowing for pulse-to-pulse variations in the ELF output, we observed the coupled power distribution to be stable. By homodyne phase measurements, we also observed that the relative phase relationship between outputs was as stable as the phase of ELF itself ($\leq \pm$ 20° pulse-to-pulse variation[11]) when averaged by 5 ns integrators. Without the integrators, the phase "noise" was $\leq \pm$ 40° during the fine-structure variations of the ELF pulse top. With the coupler installed, there was no significant change in the TE_{21}/TM_{21} mode content at the P_{SO} output as compared to that of the ELF output alone. To study arcing thresholds, the ELF output power was varied by changing the length of the resonantly excited wiggler. Being perpendicular to the microwave E-vector, we did not expect the presence of the septa to lower the arcing threshold appreciably. In addition, a previous test had demonstrated that WR-28 waveguide could handle in excess of 140 MW of power in 10-20 ns pulses without breakdown occurring. We were therefore surprised to observe evidence of arcing at an input power level of 50 to 100 MW. Power in the small coupled output guides ranged from 7 MW to 43 MW at the onset of arcing. As power was increased, the P_{SO} output power increased appropriately but the power from the four coupled outputs rapidly leveled off. The lack of suitable diagnostics and time precluded a detailed study for determinining the location of the arcing.

In the second series of tests, the septum coupler had its flanges removed, was carefully butt-welded to stainless steel waveguide extensions and placed inside the wiggler. The first septum-pair leading edges were located 1.5 m into the wiggler. This placed the septa in a high-power exponential FEL gain region. In addition to the parameters studied outside the wiggler, as described above, we wished to study the time-dependent penetration of the pulsed wiggler magnetic field into the coupler, the effect of the presence of the coupler on FEL behavior, and any changes in output third-harmonic content. Using a small, carefully positioned coil $\dot{B}$ vs t was measured at the five locations shown in Figure 6. At all of them the B risetime was $\leq$ 20 μs. This showed that no significant change in the field penetration time was introduced by the multiple walls of the coupler. General FEL behavior, e.g.gain, peak power, and beam transport, appeared unchanged by the presence of the coupler in the wiggler. The power division in the coupler and the relative phase of the five outputs was as stable as before. The TE_{21}/TM_{21} mode content and third-harmonic content also were not significantly different from their values obtained while operating the FEL without the coupler. The arcing threshold measurements, however, produced another surprise. At an active wiggler length of 1.0m, where the FEL power was only 0.6 to 0.8 MW, all four coupled outputs showed evidence of arcing. This was indicated by the detected pulse shapes reducing in width to only 2 to 3 ns (FWHM). The P_{S1} and P_{S4} power levels were 200 to 300 kw; the P_{S2} and P_{S3} levels were ~ 100 kw. These pulse shapes remained narrow and sharply peaked when the FEL power was increased to ~ 65 MW.

Inside the wiggler, of course, the septa are in an environment which includes both a magnetic field and a high current beam. The latter may have a halo or "wings" which extend to the septa leading edges. With such a ready source of electrons possibly striking the septa leading edges and causing secondary emission, an avalanching mechanism such as multipactor[12] seems a likely culprit. Instead of causing arcing, whose initiation within 2 ns is somewhat difficult to explain (the vacuum is typically $\simeq 3\times10^{-5}$ Torr), a multipactor could result in simple electron loading, i.e. absorption of the microwave power. This seems to have been confirmed by our observing an absence of power reflected back to the FEL input. Such reflections were seen during arcing when the septum coupler was located outside the wiggler. Alternative mechanisms are being considered, e.g. local high gas pressure at the septa edges which might enable a fast breakdown. In both cases, a beam-size limiter, or scraper, might eliminate the problem. Again, time did not permit further experimental studies of this power-limiting phenomenon.

A means for suppressing this effect must be found if the septum coupler is to continue being considered for a key role in the TBA. Within a year, we hope to resume coupler testing with improved diagnostics.

Acknowledgements

We are grateful for the help provided by many people: useful discussions with William Fawley, Thaddeus Orzechowski, and E.T. Scharlemann of LLNL and Robert Avery, Klaus Halbach, Kurt Kennedy and John Meneghetti of LBL; key involvement of Joseph Farmer and Howard Johnsen of Sandia, James Bryan, Richard Clouser, John Dini and Christoph Steffani of LLNL and Beverly Mecklenburg of HRC; further mechanical support by Kenneth Boyden, Wayne Cowden, Wendell Kelley, and Michael Prokosch of LLNL and G. Robert Gray, Gregory Howe, Hansrudol Krapf, and Frank Zucca of LBL; the electronics support of James Dunlap, Skip Fields and Janet Johnson of LLNL; the operational support of the ETA crew headed by James Crawford; and finally Kim Allen for the preparation of this manuscript.

References

[1] A.M. Sessler, "The Free Electron Laser as a Power Source for a High-Gradient Accelerating Structure," in Laser Acceleration of Particles, P.J. Channel ed. (AIP Conf. Proc. No. 91, American Institute of Physics, New York, 1982), p.154-159.

[2] D.B. Hopkins and R.W. Kuenning, "The Two-Beam Accelerator: Structure Studies and 35 GHz Experiments, " IEEE Trans. Nuc.Sci., NS-32, 3476-3480, October (1985).

[3] D.B. Hopkins, et.al., "High-Power 35 GHz Testing of a Free-Electron Laser and Two-Beam Accelerator Structures", Proc. of S.P.I.E. High Intensity Laser Processes Conf., 664, 61-73, Quebec City,Canada, June (1986)

[4] T.J. Orzechowski, et al, in Free Electron Generators of Coherent Radiation, C.A. Brau,S.F. Jacobs, M.O. Scully, editors (SPIE, Bellingham, WA, 1983), p. 65.

[5] R.B. Neal, editor, The Stanford Two-Mile Accelerator, W.A. Benjamin, Inc. 1968, Chap 6.

[6] J. Haimson and B. Mecklenburg, "Design and Construction of a 33 GHz Brazed Accelerator Waveguide for High Gradient Operation", these proceedings.

[7] D.B. Hopkins, et al., "Electroforming Process Development for a 33 GHz High Gradient Accelerator," these proceedings.

[8] J.C. Farmer et al., "Electroforming Process Development for the High Gradient Test Structure", Submitted to the Journal of the American Electroplater's Surface Finishers Society, also SAND 86-8959, January (1987).

[9] R.P. Wells, "Septum Coupler Vacuum Load," Internal note.

[10] D.B. Hopkins, "Septum Coupler Test Results," TBA Note 37, in preparation.

[11] T.J. Orzechowski, E.T. Scharlemann, & D.B. Hopkins, "Measurement of the Phase of the Electromagnetic Wave in a Free-Electron Laser Amplifier", Subm. to Phys. Rev. A, also UCRL - 95431, August (1986)

[12] A.J. Hatch, "Suppression of Multipacting in Particle Accelerators," Nucl. Inst. and Meth. 41, 261-271 (1966).

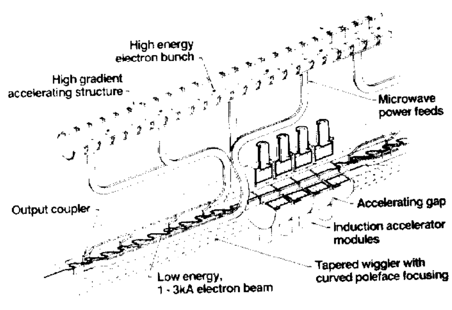

Fig. 1 Two-Beam Accelerator Concept

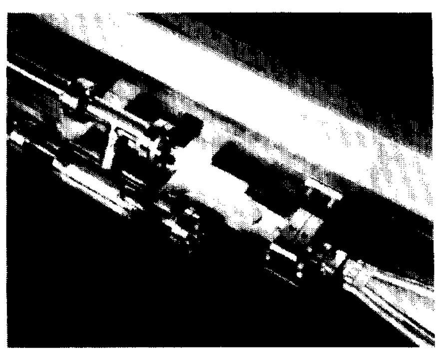

Fig. 2 Brazed HGA Assembly

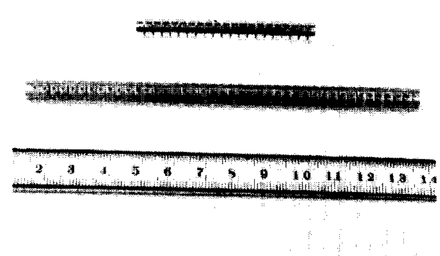

Fig. 3 Prototype Electroformed HGA and Mandrel

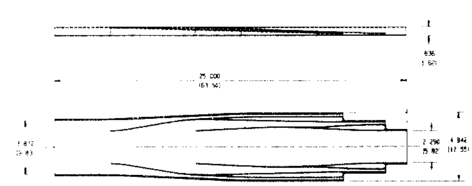

Fig. 4 Diagram of Septum Coupler Test Section

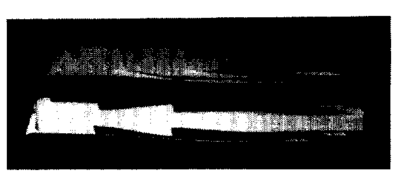

Fig. 5 Machined Septum Coupler Half

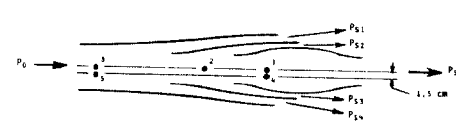

Fig. 6 Septum Coupler Test Nomenclature